




# Toxicity of nanotitanium dioxide (TiO<sub>2</sub>-NP) on human monocytes and their mitochondria

Fatemeh Ghanbary<sup>1</sup> · Enaytollah Seydi<sup>2,3</sup> · Parvaneh Naserzadeh<sup>4</sup> · Ahmad Salimi<sup>5</sup> 

Received: 25 September 2017 / Accepted: 6 December 2017 / Published online: 20 December 2017  
© Springer-Verlag GmbH Germany, part of Springer Nature 2017

## Abstract

The effect of nanotitanium dioxide (TiO<sub>2</sub>-NP) in human monocytes is still unknown. Therefore, an understanding of probable cytotoxicity of TiO<sub>2</sub>-NP on human monocytes and underlining the mechanisms involved is of significant interest. The aim of this study was to assess the cytotoxicity of TiO<sub>2</sub>-NP on human monocytes. Using biochemical and flow cytometry assessments, we demonstrated that addition of TiO<sub>2</sub>-NP at 10 µg/ml concentration to monocytes induced cytotoxicity following 12 h. The TiO<sub>2</sub>-NP-induced cytotoxicity on monocytes was associated with intracellular reactive oxygen species (ROS) generation, mitochondrial membrane potential (MMP) collapse, lysosomal membrane injury, lipid peroxidation, and depletion of glutathione. According to our results, TiO<sub>2</sub>-NP triggers oxidative stress and organelles damages in monocytes which are important cells in defense against foreign agents. Finally, our findings suggest that use of antioxidants and mitochondrial/lysosomal protective agents could be of benefit for the people in the exposure with TiO<sub>2</sub>-NP.

**Keywords** TiO<sub>2</sub>-NP · Monocytes · Cytotoxicity · Mitochondrial damage · Oxidative stress

## Introduction

Particles of TiO<sub>2</sub>-NPs were categorized as biologically inert in both human and animals (Ghosh et al. 2013). According to the US National Nanotechnology Initiative, TiO<sub>2</sub>-NPs are the most produced and are widely used in a broad range of products such as food colorants, cosmetics, and sunscreen (Jin

et al. 2008). The behavior and environmental fate of TiO<sub>2</sub>-NPs is a quickly expanding area of research. Generation of TiO<sub>2</sub>-NPs was an appraised 1.45 million metric tons per year. The number of US workers exposed to TiO<sub>2</sub>-NPs dust is not existing. TiO<sub>2</sub>-NPs are manufactured and used in the workplace in ranging of particle size fractions including nanoparticles, ultrafine and fine (Lai et al. 2008). Because of the small size of nanoparticles simplified their uptake into cells as well as across epithelial cells into lymph and finally blood circulation (Gheshlaghi et al. 2008), TiO<sub>2</sub>-NPs can not only arrive cells, but also arrive mitochondria and nuclear (Gheshlaghi et al. 2008).

There is an increasing number of reports indicating potential toxic of TiO<sub>2</sub>-NPs (Jin et al. 2008, Vevers and Jha 2008). Lai and co-workers demonstrated that TiO<sub>2</sub>-NPs are toxic for human neural cells and fibroblasts (Lai et al. 2008). Previous studies reported that TiO<sub>2</sub>-NPs reduced cell viability, mitochondrial function, changed cell morphology, and apoptosis in JB6 cells (Zhao et al. 2009). Moreover, Manosij Ghosh and colleagues using an ex vivo model of human erythrocyte and lymphocyte cells proposed that these particles could induce a significant reduction in mitochondrial dehydrogenase activity DNA damage and apoptosis in a dose-dependent manner in human lymphocyte cells (Ghosh et al. 2010). It was also pointed out that TiO<sub>2</sub>-NPs changed cell morphology, increased

---

Responsible editor: Philippe Garrigues

---

✉ Parvaneh Naserzadeh  
pnnew2011@yahoo.com

✉ Ahmad Salimi  
salimikd@yahoo.com; a.salimi@pharmacy.arums.ac.ir

<sup>1</sup> Department of Chemistry, Mahabad Branch, Islamic Azad University, Mahabad, Islamic Republic of Iran

<sup>2</sup> Research Center for Health, Safety and Environment (RCHSE), Alborz University of Medical Sciences, Karaj, Iran

<sup>3</sup> Department of Occupational Health Engineering, Alborz University of Medical Sciences, Karaj, Iran

<sup>4</sup> Department of Pharmacology and Toxicology, Faculty of Pharmacy, Shahid Beheshti University of Medical Sciences, Tehran, Iran

<sup>5</sup> Department of Pharmacology and Toxicology, School of Pharmacy, Ardabil University of Medical Science, P.O. Box: 56189-53141, Ardabil, Iran

oxidative stress, and decreased proliferation on cells constitutive of alveolo-capillary barrier in vitro (Hanot-Roy et al. 2016).

The TiO<sub>2</sub>-NPs were studied for cytotoxicity and mechanism of action on human monocytes and their isolated mitochondria. Cellular parameters such as reactive oxygen species (ROS) generation, mitochondrial membrane potential (MMP) collapse, lysosomal membrane injury, lipid peroxidation depletion of glutathione, ADP/ATP ratio, and mode of cell death were evaluated using flow cytometry and mitochondria parameters such as succinate dehydrogenases activity (SDH), ROS generation, mitochondrial swelling, and cytochrome c release. Morphological alterations of erythrocytes and changes in their hemolytic properties and interaction with hemoglobin were also examined.

## Materials and methods

### Nanoparticle preparation

To get nanostructured TiO<sub>2</sub>, 12 ml Ti (OC<sub>3</sub>H<sub>7</sub>)<sub>4</sub> solution was dissolved in 1.35 ml MeOH, and the mixture was sonicated for 3 min and shaken at 70 °C for 210 min under magnetic stirrer. Then, water was added dropwise into the hot solution (70 °C) during this period. The precipitate was isolated by filtration and washed with hot water and organic solvents to remove the adsorbed impurities and then calcined at different temperatures for 3 h. The crystal structure of the powders was checked by powder X-ray diffraction (XRD) using Siemens X-ray diffraction D5000 with Cu K $\alpha$  radiation. An accelerating voltage of 40 kV and an emission current of 30 mA were used<sup>6</sup>. The average crystalline size of the samples was calculated according to the Debye-Scherrer formula<sup>28</sup>:

$$D = \frac{0.89\lambda}{\beta \cos\theta}$$

where  $D$  (Å) is the average crystallite size,  $\lambda$  is the wavelength of the X-ray radiation (Cu K $\alpha$  = 1.54178 Å),  $\beta$  is the full width at half maximum intensity of the peak, and  $\theta$  is the diffraction angle. If a sample contains anatase and rutile forms, the mass fraction of rutile ( $\chi$ ) can be calculated from the following equation<sup>29</sup>:

$$\chi = \frac{IR}{0.8IA + IR}$$

IA and IR represent the integrated intensity of the anatase (101) and rutile (110) peaks, respectively. Scanning electron microscopy (SEM) of samples was carried out on a Philips XL 30 microscope. The morphology and grain size of TiO<sub>2</sub> nanopowders were investigated by transmission electron microscopy (TEM) on a Philips CM operating at 200 kV.

## Cellular assessments

### Blood samples

All blood samples ( $n = 10$ ) were acquired and approved by Blood Administration Center. The studies were performed at the School of Pharmacy, Shahid Beheshti University of Medical Sciences; the health of donor was confirmed by an expert physician. This study was approved by the Shahid Beheshti University of Medical Sciences research ethics committee, and all healthy individuals signed an informed consent form.

### Monocyte isolation

Peripheral human blood monocytes were separated from heparinized blood samples. Briefly, blood samples were diluted in calcium and magnesium free Hanks balanced solution. The diluted blood was layered over Ficoll Hypaque in a 2:1 ratio and centrifuged at 400 $\times g$  for 20 min at 4 °C. The mononuclear cell interface was removed and washed by repeated centrifugations to remove Ficoll contamination, platelets, and residual erythrocytes. Mononuclear cells were counted and adjusted to 10<sup>6</sup> cells/ml and suspended into 96-well microplates. The monocytes were isolated by their adherent capacity, followed by 1-h incubation at 37 °C in humidified 95% O<sub>2</sub> and 5% CO<sub>2</sub>. Isolated monocytes were cultured in RPMI-1640 supplemented with 10% pooled human AB serum, 100 units/ml penicillin, 100 mg/ml streptomycin, and 2 mmol/l glutamine (Vahid et al. 2004).

### MTT assay

Monocytes were seeded in 96-well plates (10<sup>3</sup>/well), exposed to TiO<sub>2</sub>-NPs (0, 10, 20, 50, and 100  $\mu\text{g/ml}$ ). After 12 h incubation, MTT reagent was added to the wells and after 2-h incubation at 37 °C, absorbance was measured in a plate reader (Tecan, Rainbow Hermo, Austria) at 580 nm (Salimi et al. 2017).

### Determination of ROS

To determine the rate of monocytes ROS generation, dichlorofluorescein diacetate (DCFH-DA, 1.6  $\mu\text{M}$ ) was added to the monocytes. It penetrates monocytes and becomes hydrolyzed to non-fluorescent dichlorofluorescein (DCFH). The latter then reacts with ROS to form the highly fluorescent dichlorofluorescein (DCF), which effluxes the cell. The fluorescence intensity of DCF was measured using a BD flow cytometry, and data were analyzed by flowing software. The results were expressed as fluorescent intensity per 10<sup>6</sup> cells (Salimi et al. 2016b).

## MMP assay

Mitochondrial uptake of the cationic fluorescent dye, rhodamine 123 (1.5  $\mu\text{M}$ ), has been used for the estimation of mitochondrial membrane potential. The amount of rhodamine 123 remaining in the incubation medium was measured using a BD flow cytometry, and data were analyzed by flowing software. The capacity of mitochondria to take up the rhodamine 123 was calculated as the difference (between control and treated cells) in rhodamine 123 fluorescence (Salimi et al. 2016b).

## Lysosomal membrane integrity assay

Monocyte lysosomal membrane stability was determined from the redistribution of the fluorescent dye, acridine orange. Aliquots of the cell suspension (0.5 ml) that were previously stained with acridine orange (5  $\mu\text{M}$ ) were separated from the incubation medium by 1 min centrifugation at 1000 rpm. Cell washing process was carried out twice to remove the fluorescent dye from the media. Acridine orange redistribution in the cell suspension was then measured using a BD flow cytometry, and data were analyzed by Flowing software 2.5.1 (Salimi et al. 2016b).

## Lipid peroxidation

Evaluation of lipid peroxidation in monocytes was conducted by determining the amount of thiobarbituric acid reactive substances (TBARS) formed during the decomposition of lipid hydroperoxides by following the absorbance at 532 nm in a Beckman DU-7 spectrophotometer (Salimi et al. 2016b).

## GSH and GSSG

GSH and GSSG were measured pursuant to the spectrofluorometric procedure (Hissin and Hilf 1976). Each sample was evaluated in quartz cuvettes usage a fluorimeter set at 350 nm excitation and 420 nm emission wavelengths.

## ADP/ATP ratio assay

Changes in the ADP/ATP ratio have been used to differentiate modes of cell death and viability. ADP/ATP ratio was assessed by ADP/ATP Ratio Assay kit (MAK135 Sigma, USA) in monocytes using luminometer. ADP/ATP ratio was performed according to the manufacturer's instructions (Salimi et al. 2015a).

## Apoptosis versus necrosis assay

Apoptosis and necrosis were assessed by flow cytometric analysis (BD flow cytometry and data were analyzed by

Flowing software 2.5.1) of Annexin V-fluorescein isothiocyanate (FITC)/propidium iodide (PI) stained cells. Annexin V/PI assay was performed using a commercial kit (Immunotech; Beckman Coulter) according to the manufacturer's instructions (Salimi et al. 2015b).

## Mitochondrial assessments

### Monocytes lysis and isolation of mitochondria

Mitochondria were isolated from the monocytes by mechanical lysis and differential centrifugation. Briefly, monocytes were washed with cold PBS at 4 °C and centrifuged at 450 $\times$ g. The pellet was resuspended in cold isolation buffer (75 mmol/l sucrose, 20 mmol/l HEPES, 225 mmol/l mannitol, 0.5 mmol/l EDTA, pH 7.2), and the cells were disrupted by homogenization. Non-lysed monocytes and nuclei were spun down by centrifugation at 750 $\times$ g for 20 min. The supernatant was further spun at 10,000 $\times$ g for 10 min twice. The pellet, designated as the mitochondrial fraction, was suspended in assay buffer (140 mmol/l KCl, 10 mmol/l NaCl, 2 mmol/l  $\text{MgCl}_2$ , 0.5 mmol/l  $\text{KH}_2\text{PO}_4$ , 20 mmol/l HEPES, 0.5 mmol/l EGTA; adjusted to pH 7.2 with KOH) (Rotem et al. 2005; Salimi et al. 2015b). Protein concentrations were measured through the Coomassie blue protein-binding protocol as explained by Bradford (Bradford 1976). For the normalization, the mitochondrial samples (0.5 mg mitochondrial protein/ml) were used.

### Succinate dehydrogenases activity

Complex II enzyme activity was measured by Complex II Enzyme Activity Microplate Assay Kit (ab109908, UK). Each well in the kit has been coated with an anti-complex II monoclonal antibody (mAb) which purifies the enzyme from a complex sample. After this in-well purification, the production of ubiquinol by the enzyme is coupled to the reduction of the dye DCPIP (2,6-dichlorophenolindophenol) and a decrease in its absorbance at 600 nm, which in turn recycles the substrate ubiquinone (Salimi et al. 2015c).

### Mitochondrial swelling assay

Mitochondria suspensions (at 100  $\mu\text{g}$  protein per well) were incubated in 96-well plates at 25 °C in swelling buffer (140 mmol/l KCl, 10 mmol/l NaCl, 2 mmol/l  $\text{MgCl}_2$ , 0.5 mmol/l  $\text{KH}_2\text{PO}_4$ , 20 mmol/l HEPES, 0.5 mmol/l EGTA; adjusted to pH 7.2 with KOH) supplemented with 1 mg/ml rotenone and 10 mmol/l succinate. Mitochondrial swelling was measured spectrophotometrically in duration 1 h. Mitochondrial swelling results in a decrease in absorbance monitored at 540 nm (Talari et al. 2014).

## Cytochrome C release assay

The concentration of cytochrome C was measured by the Quantikine Human Cytochrome C Immunoassay kit (Minneapolis, Minn). Cytochrome C evaluation was accomplished pursuant to the manufacturer's instructions (Salimi et al. 2016a).

## ICP-MS analysis

Nanoparticles in the monocytes were determined by inductively coupled plasma mass spectrometry (ICP-MS). Briefly, cells were exposed for 3, 6, and 12 h to TiO<sub>2</sub>-NPs in a concentration 25 µg/ml and washed twice with PBS to remove particles loosely bound to the cell surface. The cells were digested with nitric acid (1 M) and perchloric acid (1 M) (at a ratio of 4:1 v/v) for 48 h and were incubated at 120 °C (to remove the remaining acids). Each sample was diluted with distilled water (1 ml) and used for TiO<sub>2</sub>-NPs total mass ICP-MS (Varian Vista-Pro, Australia) (Böhme et al. 2014).

## Statistical analysis

Results were presented as mean ± SEM. Assays were performed in triplicate and the mean was used for statistical analysis. Statistical significance was determined using the Student's *t* test. All graphs were expressed as mean ± SEM, and *P* < 0.05 was considered statistically significant. Flow cytometry data were analyzed by Flowing software.

## Results

### Purity and morphological characteristics of nanoparticles

As shown in Fig. 1a, at 400 °C, the anatase phase was formed. Catalytic activity of mesoporous TiO<sub>2</sub> is strongly dependent on its phase structure, crystallite size, and pore structure. It is well known that anatase type TiO<sub>2</sub> has higher catalytic activity than rutile type TiO<sub>2</sub>. In anatase phase, the samples with small grain size have higher catalytic activity than the others, which

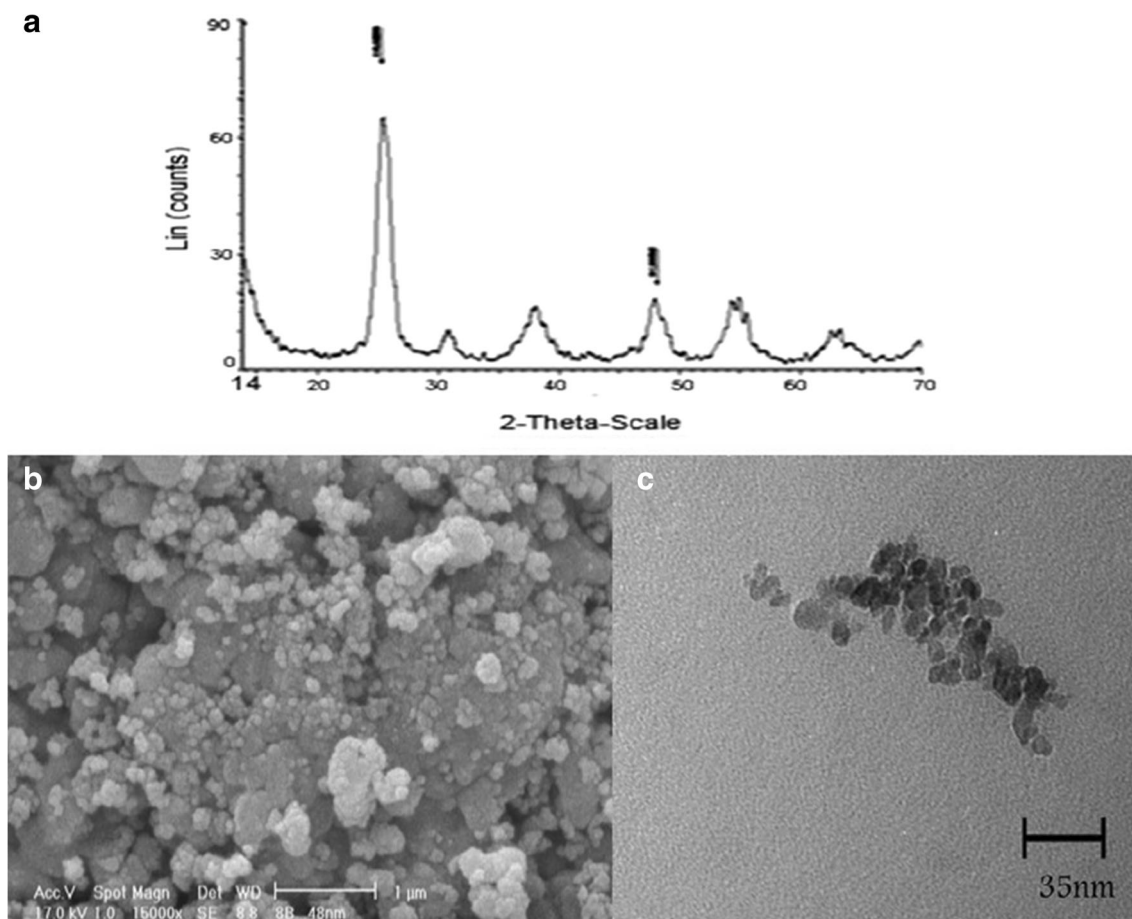


**Fig. 1** X-ray diffraction patterns of TiO<sub>2</sub> nanopowders calcinated at 400 °C (a). SEM images of TiO<sub>2</sub> nanopowders calcinated at 400 °C (b). TEM images of TiO<sub>2</sub> nanopowders calcinated at 400 °C (c)

also is consistent with the experimental results. XRD method has been performed on a powdered compound, and the particle size ( $L$ ) was estimated using Debye-Scherrer formula:

$$L = \frac{K \times \lambda}{\Delta(2\theta) \times \cos(\theta)}$$

$K$  is the form factor (equal to 0.9),  $\lambda = 0.15418$  nm,  $2\theta$  is the peak position, and  $\Delta(2\theta)$  is the full width at half maximum of the diffraction peak in terms of radians. Using this formula, particle size was estimated to be 20 nm. Catalytic

activity of mesoporous  $\text{TiO}_2$  is strongly dependent on its phase structure, crystallite size, and pore structure. It is well known that anatase type  $\text{TiO}_2$  has higher catalytic activity than rutile type  $\text{TiO}_2$ . Moreover, in the anatase phase, the samples with small grain size have higher photocatalytic activity than the others, which also is consistent with the experimental results. Therefore, we used this type of powder in this research.

The prepared titania nanopowders were characterized by scanning electron microscopy (SEM) (Fig. 2b). Several synthesis conditions have been assayed. When  $\text{TiO}_2$  powders is

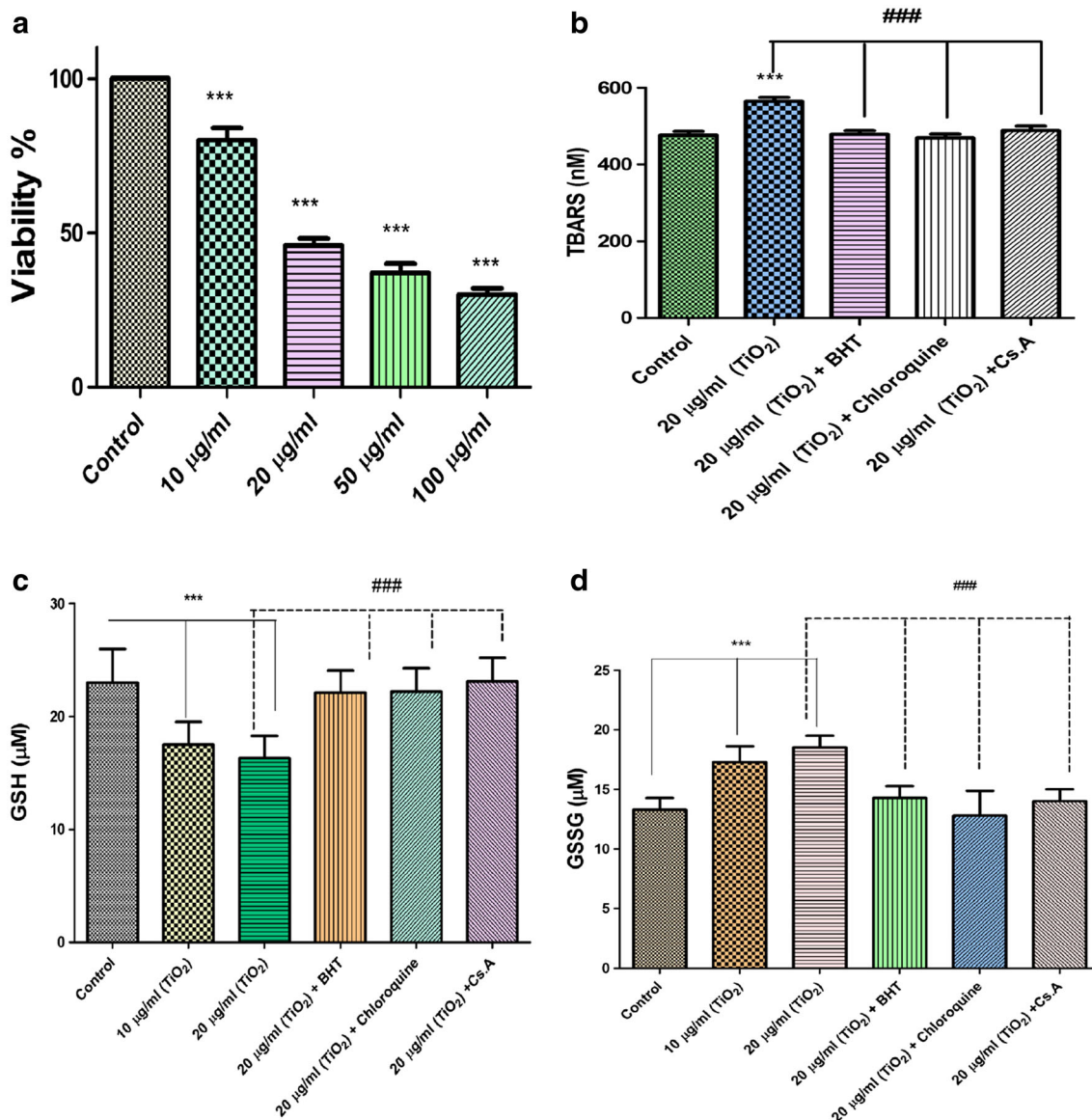


**Fig. 2** Cell viability (a); human monocytes from healthy donors, at  $1 \times 10^4$  cells/well, were seeded on 96-well plates.  $\text{TiO}_2$ -NPs at 10–100  $\mu\text{g/ml}$  concentrations were incubated for 12 h. The absorbance representing the viability of human monocytes was determined by the ELISA reader at 570 nm. Lipid peroxidation (b) monocytes ( $10^6$  cells/ml) were incubated in the RPMI 1640 at 37 °C for 6 h following the addition of  $\text{TiO}_2$ . TBARS formation was expressed as nM concentrations. GSH and GSSG (C)

monocytes ( $10^6$  cells/ml) were incubated in the RPMI 1640 at 37 °C for 6 h following the addition of  $\text{TiO}_2$ . Intracellular GSH (C) and extra cellular GSSG (D) were fluorometrically determined. Values are expressed as mean  $\pm$  SD of three separate experiments ( $n = 5$ ). Significant difference in comparison with untreated control (\*\*\*)  $P < 0.001$ . Significant difference in comparison with  $\text{TiO}_2$ -NPs-treated monocytes and preventive agent (###)  $P < 0.001$

calcinated at high temperatures (~400 °C), crystal structure transformations may occur. The amorphous-anatase and anatase-rutile transitions depend strongly on the calcination conditions. The prepared titania powder was characterized by TEM (Fig. 2c).

### Cell viability

Our results showed that TiO<sub>2</sub>-NPs are capable significantly to reduce viability of monocytes within 12 h at concentrations of 10, 20, 50, and 100 µg/ml. As shown in Fig. 1, cytotoxicity was seen, 20, 54, 63, and 69%, in treated monocytes with TiO<sub>2</sub>-NPs at concentrations of 10, 20, 50, and 100 µg/ml, respectively. Inhibitory concentration (IC<sub>50</sub>) was almost 25 µg/ml (Fig. 2a).

### Lipid peroxidation

As shown in Fig. 2, a significant amount of TBARS was formed when incubated with TiO<sub>2</sub>-NPs at concentration of 20 µg/ml. TiO<sub>2</sub>-NP-induced TBARS formation was prevented by ROS scavenger (butylated hydroxytoluene (BHT) 50 µM), mitochondrial permeability transition (MPT) pore sealing agent (cyclosporine A (Cs.A) 5 µM), and chloroquine as a lysosomotropic agent (Fig. 2b).

### GSH and GSSG

As indicated in Fig. 2c, d, incubation of monocytes with TiO<sub>2</sub>-NPs induced rapid monocytes GSH depletion at concentrations of 10 and 20 µg/ml. Most of the TiO<sub>2</sub>-NP-induced GSH depletion may be related to the dismissal of GSSG (Fig. 2c). Again, MPT pore sealing agents (Cs.A), lysosomotropic agents (chloroquine), and antioxidant (BHT) significantly prevented both TiO<sub>2</sub>-NP-induced intracellular GSH decrease and extracellular GSSG increase (Fig. 2d). All of these reagents did not create any significant effects on monocytes GSH/GSSG status at concentrations used (data not shown).

### ROS formation

The results of the ROS measurement showed that the ratio of reactive oxygen radical, after exposure to TiO<sub>2</sub>-NPs, significantly increased at lower concentrations (5, 10, and 20 µg/ml) and time intervals (2, 4, and 6 h). As shown in Fig. 3a, BHT as an antioxidant agent significantly reduced ROS formation in compared to 20 µg/ml of TiO<sub>2</sub>-NPs. H<sub>2</sub>O<sub>2</sub> was used as a positive control for assessment of ROS formation.

### MMP collapse

Our result showed that TiO<sub>2</sub>-NPs in all time (2, 4, and 6 h) at concentrations 5, 10, and 20 µg/ml significantly decreased the MMP collapse. Concurrent use of MPT pore sealing agents (Cs.A) combined with TiO<sub>2</sub>-NPs (20 µg/ml) led to decrease mitochondrial damage and inhibition of MMP collapse. Ca<sup>+2</sup> was used as a positive control for assessment of MMP collapse (Fig. 3b).

### Lysosomal integrity

The results showed that TiO<sub>2</sub>-NPs at higher used concentrations (20 µg/ml) could cause lysosomal membrane damage in time intervals (2, 4, and 6 h). Concurrent use of lysosomal protective (chloroquine) combined with TiO<sub>2</sub>-NPs at concentration of 20 µg/ml led to decrease lysosomal damage and inhibition of rupture of lysosomal membrane (Fig. 3c).

### ADP/ATP ratio

ATP and ADP were measured using bioluminescence based on luciferin/luciferase reaction. The ADP and ATP were measured at 3 and 6 h in monocytes following exposure with or without TiO<sub>2</sub>-NPs (20 µg/ml) (Table 1). As shown in Table 1, TiO<sub>2</sub>-NPs significantly ( $P < 0.0001$ ) decreased ATP and increased ADP following exposure of monocytes.

### Apoptosis and necrosis

As show in Fig. 4, the apoptosis was quantified by the externalization of PS (phosphatidylserine), assessed by Annexin V-PI double staining at 6 h. The percentage of apoptotic cells was determined as 6.99% at 6 h in monocytes after exposure with 20 µg/ml TiO<sub>2</sub>-NPs, which is significantly ( $P < 0.001$ ) higher than that of control at 6 h (Fig. 4).

### SDH activity

Evaluation of TiO<sub>2</sub>-NPs for potential activity on mitochondria obtained from monocytes was carried out by studying the inhibitory effects of this compound on SDH activity using Complex II Enzyme Activity Microplate Assay Kit. TiO<sub>2</sub>-NPs inhibited succinate dehydrogenase activity in isolated mitochondria at the low concentrations (2.5 to 20 µg/ml) (Fig. 5a).

### Mitochondrial swelling

Mitochondrial swelling has been considered as an indication of the opening of the MPTP, which results in depolarization of mitochondrial membrane potential. We observed that

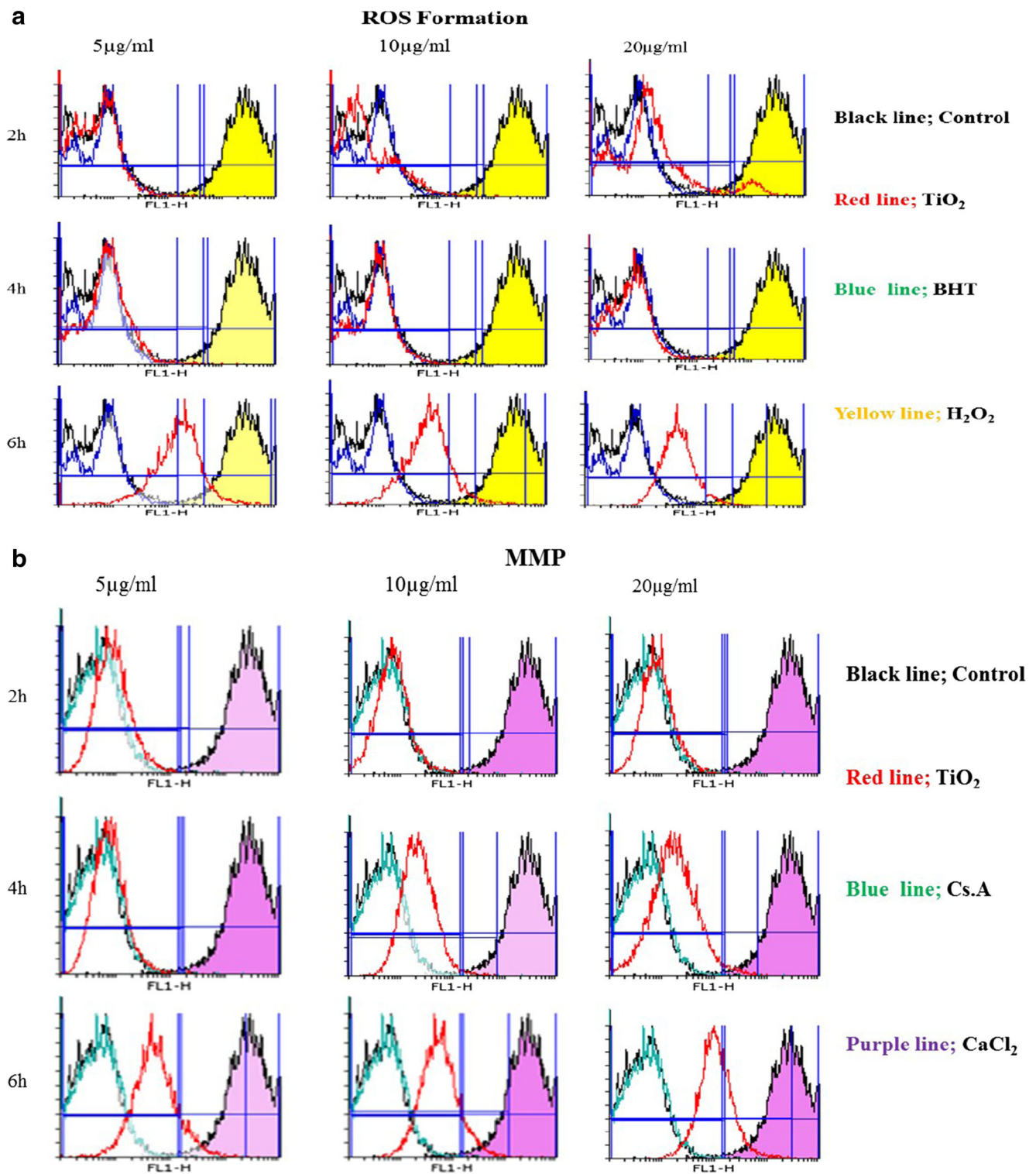


**Fig. 3** Effects of TiO<sub>2</sub>-NPs on intracellular ROS formation (a), MMP collapse (b), and lysosomal integrity damage (c) in monocytes. TiO<sub>2</sub>-NP-induced ROS generation in monocytes. **a** The value 10<sup>6</sup> cells/ml was either not treated (black line) or treated with TiO<sub>2</sub>-NPs (red line), TiO<sub>2</sub>-NPs + BHT (blue line), and H<sub>2</sub>O<sub>2</sub> as a positive control (yellow line) for time interval 2–6 h. The cells were loaded with the fluorescent probe DCF-DA. Upon ROS formation, the fluorescence becomes weaker and the peak moves to the left. **b** The value 10<sup>6</sup> cells/ml was either not treated (black line) or treated with TiO<sub>2</sub>-NPs (red line), TiO<sub>2</sub>-NPs + Cs. A (green

line), and CaCl<sub>2</sub> as a positive control (purple line) for time interval 2–6 h. The cells were loaded with the fluorescent probe rhodamine 123. Upon mitochondrial membrane depolarization, the fluorescence becomes weaker and the peak moves to the left. **c** TiO<sub>2</sub>-NP-induced lysosomal integrity damage in monocytes. The value 10<sup>6</sup> cells/ml was either not treated (black line) or treated with TiO<sub>2</sub>-NPs (red line) and TiO<sub>2</sub>+ chloroquine (green line) for time interval 2–6 h. The cells were loaded with the fluorescent probe acridine orange

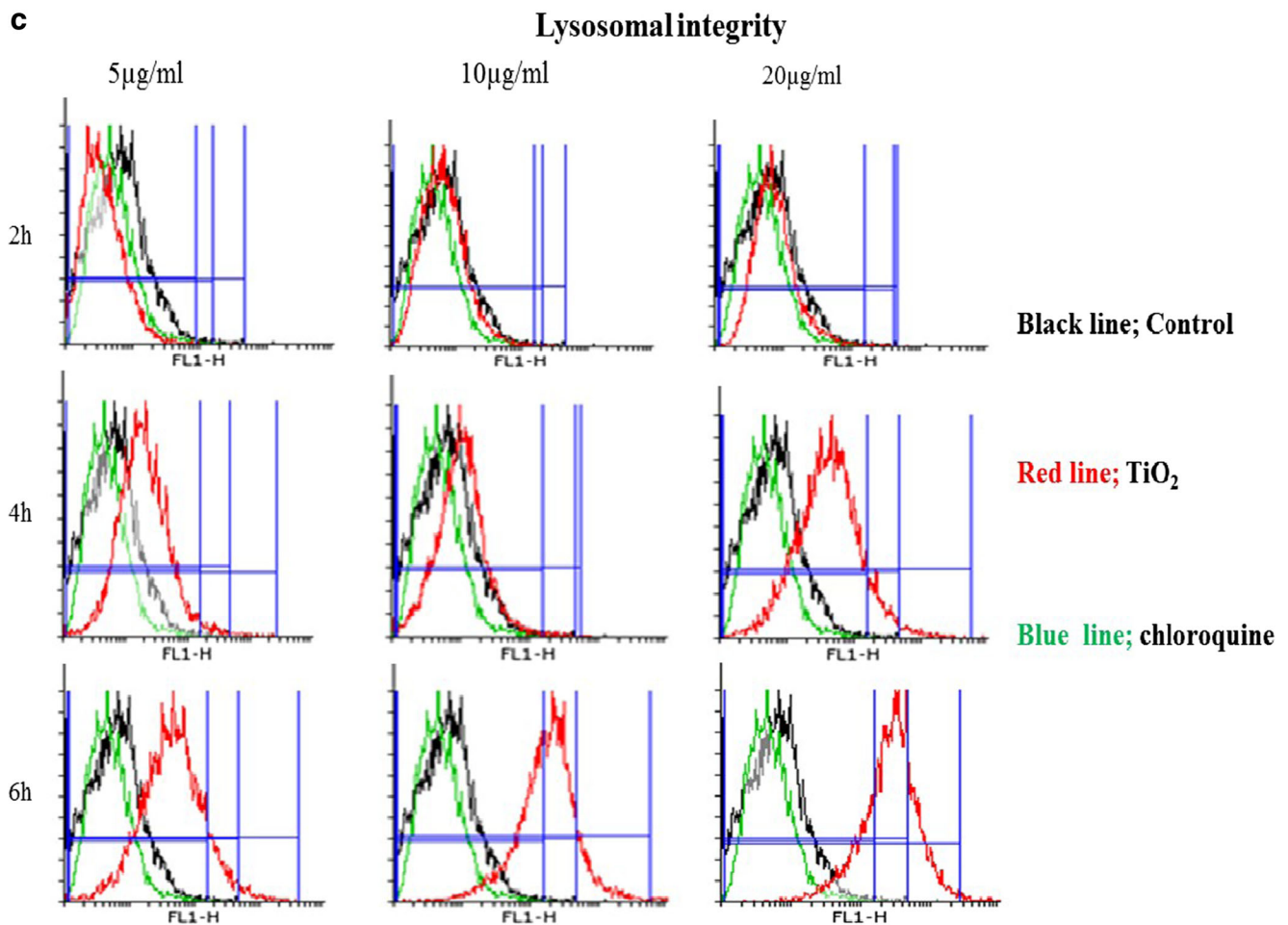


**Fig. 3** (continued)

mitochondrial swelling was induced at the middle concentrations (2.5, 5, and 10 μg/ml). We also recorded mitochondrial

membrane potential using rhodamine 123 and ROS formation using DCF-DA after treatment with TiO<sub>2</sub>-NPs (data not shown) (Fig. 5b).

**Table 1** Content of ATP and ADP at 0, 3, and 6 h in the absence and presence TiO<sub>2</sub>-NPs in monocytes

	nmol/mg protein	
	Human monocytes	
	Control	20 μg/ml TiO <sub>2</sub>
ATP 0 h	13.33 ± 0.38	13.15 ± 0.43
ADP 0 h	2.40 ± 0.025	2.38 ± 0.02
ATP 3 h	13.04 ± 0.32	11.15 ± 0.21 <sup>a</sup>
ADP 3 h	2.37 ± 0.08	3.37 ± 0.04 <sup>b</sup>
ATP 6 h	13.34 ± 0.07	9.31 ± 0.02 <sup>a</sup>
ADP 6 h	2.38 ± 0.14	4.3 ± 0.21 <sup>b</sup>

Results were analyzed using Student's *t* test

<sup>a</sup> ATP significantly ( $P < 0.05$ ) decreased compared with control group in each time

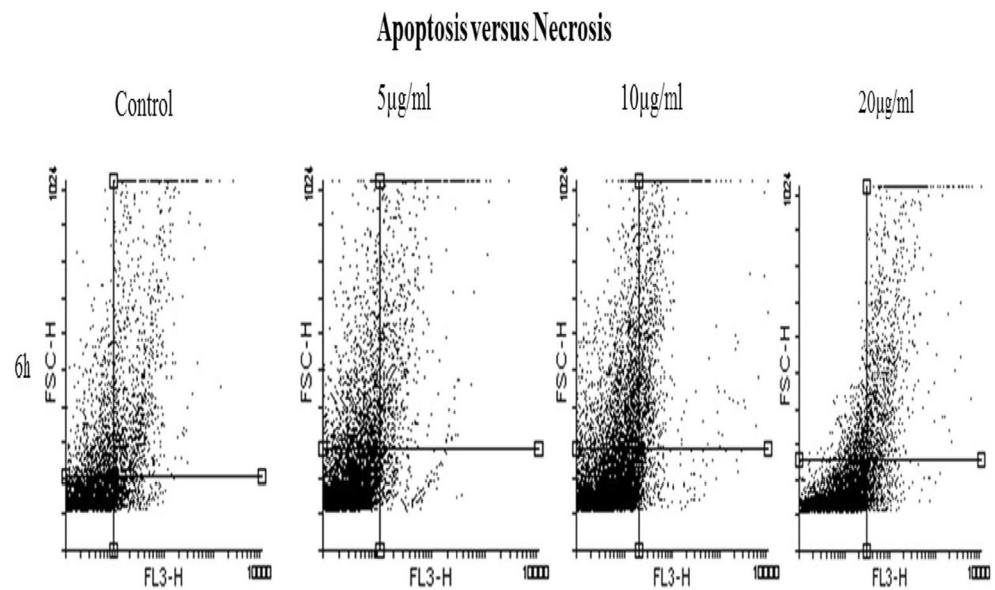
<sup>b</sup> ADP significantly ( $P < 0.05$ ) increased compared with control group in each time

### Cytochrome C release

The process of cell death involves the release of cytochrome C from the mitochondria, which eventually causes apoptotic cell death. Our results indicated that TiO<sub>2</sub>-NPs significantly caused collapse of the mitochondrial membrane potential and mitochondrial swelling (data not shown) in isolated mitochondria. These events could lead to mitochondrial permeability transition and release of cytochrome C into the cytosolic fraction. As shown in Fig. 5c, TiO<sub>2</sub>-NPs at 5 μg/ml enforced significant ( $P < 0.05$ ) release of cytochrome C. Significantly, the pretreatment of TiO<sub>2</sub>-NP-treated mitochondria with the MPT inhibitors of Cs.A and BHT, an antioxidant, inhibited cytochrome C release as compared with treated group (500 μM) ( $P < 0.05$ ), representing the role of oxidative stress and MPT pore opening in cytochrome C release (Fig. 5c).



**Fig. 4** Effect of TiO<sub>2</sub>-NPs on apoptosis and necrosis%. Early apoptosis was measured at 6 h. TiO<sub>2</sub>-NPs induced apoptosis in monocytes in compared to control. Results are expressed as means  $\pm$  SD,  $n = 5$



## Cell uptake

Cell uptake was determined by ICP-MS analysis. Our results showed that TiO<sub>2</sub>-NP levels significantly ( $P < 0.001$ ) increased in monocytes after exposure with nanoparticles at concentration 25  $\mu\text{g/ml}$  in interval times 3, 6, and 12 h (Fig. 5d).

## Discussion

TiO<sub>2</sub>-NPs can enter the body through many ways, after which it enters the blood circulation and is deposited in organs, changing biochemical indicators and causing toxicity (Hong and Zhang 2016). Our results showed that TiO<sub>2</sub>-NPs are toxic for human monocytes at concentrations of 10  $\mu\text{g/ml}$  and higher concentrations (Fig. 2a). TiO<sub>2</sub>-NPs have been recognized as a biocidal agent against a broad range of harmful microorganisms through formation of ROS (Wu et al. 2010; Yu et al. 2013). Exposure to ROS derived from TiO<sub>2</sub>-NPs has raised concerns because ROS are believed to play an important role in many inflammatory skin disorders, skin aging, and cancer formation (He et al. 2005). Our results showed that TiO<sub>2</sub>-NPs caused statistically increase in ROS formation in human monocytes and their isolated mitochondria (Fig. 3a). We also found that TiO<sub>2</sub>-NPs caused significant oxidative damage to lipids in human monocytes after 6 h incubation. The obtained results may be explained by the fact that TiO<sub>2</sub>-NPs most strongly generated ROS in human monocytes at used concentration (Fig. 3).

Excessive production of ROS breaks the balance of the oxidant/antioxidant system, resulting in lipid peroxidation and cell apoptosis. This process may contribute to decreased activity for antioxidant enzymes such as SOD, CAT, and

GSH-Px, as well as non-enzyme antioxidants such as and glutathione (GSH) (Liu et al. 2010). Our results indicate that at the used concentrations, TiO<sub>2</sub>-NPs could induce MMP collapse in intact monocytes and their isolated mitochondria; the latter inhibited by BHT as an antioxidant agent which reflects the role of ROS formation in mitochondrial damages. Cell culture experiments showed that TiO<sub>2</sub>-NPs may exacerbate inflammation and apoptosis, inhibit the cell cycle and energy metabolism, and cause the generation of ROS (Long et al. 2007). Moreover, TiO<sub>2</sub>-NPs also have an effect on the mitochondrial membrane (Cui et al. 2010; Hussain et al. 2010; Natarajan et al. 2015). Our studies showed that mitochondria are the targeted organelle of TiO<sub>2</sub>-NPs, which reduce the mitochondrial membrane proteins, ROS formation, and mitochondrial swelling and led to cytochrome c release and eventually, apoptosis (Fig. 3b).

Since many lysosomes are rich in redox-active Fe<sup>2+</sup>/Fe<sup>3+</sup> due to degradation of iron-containing macromolecules, Fenton-type reactions then take place resulting in lysosomal membrane rupture with release of powerful lytic enzymes. We showed that TiO<sub>2</sub>-NPs damaged to lysosomal integrity in human monocytes. Our results showed that with use of antioxidant and MPT pore sealing agents, lysosomal damage is inhibited (Fig. 3c).

Cell necrosis results from release of cell components to the extracellular medium and disruption of the cell membrane, while apoptosis is distinguished by condensation of nuclear chromatin and cell shrinkage followed by nuclear fragmentation. Unlike necrotic cells, apoptotic cells are quickly phagocytized without triggering inflammatory reactions. It is compulsory to characterize whether cell death is either necrotic or apoptotic because these processes have different biological importance. Our results showed that TiO<sub>2</sub>-NPs induced both form of cell death in human monocytes (Fig. 4).

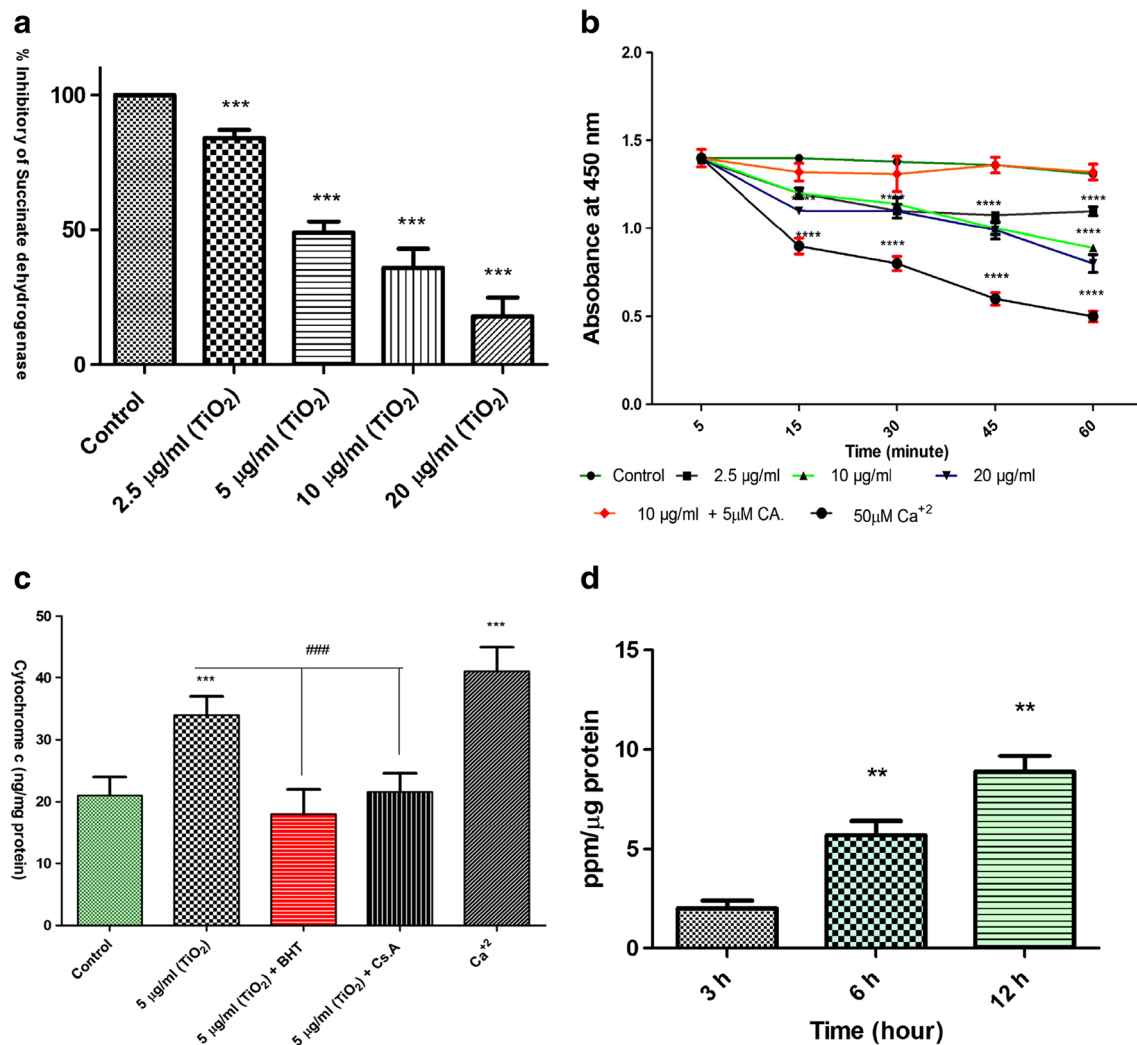


**Fig. 5** The effect of TiO<sub>2</sub>-NPs on SDH in mitochondria (a). SDH activity was evaluated following 1 h of treatment (a). SDH activity significantly ( $P < 0.001$ ) decreased by TiO<sub>2</sub>-NPs in the mitochondria. Mitochondrial swelling (b). Addition of TiO<sub>2</sub>-NPs (2.5, 5, and 10 µg/ml) induces mitochondrial swelling in monocyte mitochondria. The mitochondrial swelling was measured by following absorbance ( $\lambda_{\max} = 540$  nm) decrease. Effect of TiO<sub>2</sub>-NPs on the cytochrome c release in mitochondria (c). The amount of expelled cytochrome c from mitochondrial fraction into the suspension buffer was determined using human cytochrome c ELISA kit. TiO<sub>2</sub>-NPs significantly induced

cytochrome c release in comparison with control. As shown in this figure, pretreatment with BHT and Cs. A significantly inhibited cytochrome c release in the mitochondria. Values presented as mean  $\pm$  SD ( $n = 5$ ). Triple asterisks indicate significance in comparison with control group. Triple number signs indicate significance in comparison with TiO<sub>2</sub>-NP group. The cell uptake of TiO<sub>2</sub>-NPs (d). ICP-MS analysis proved absence of TiO<sub>2</sub>-NPs in monocyte after exposure with concentration of 25 µg/ml in interval times 3, 6, and 12. Double asterisks indicate significance in comparison with 3 h ( $n = 3$ )

Mitochondria perform significant roles in cellular energy metabolism, free radical generation, control of cell death, growth, development, integration of signals from mitochondria to nucleus and nucleus to mitochondria, and various metabolic pathways (Singh et al. 2014). The assessment time for mitochondrial toxicity parameters was selected according to previous studies (1 h) (Hosseini et al. 2013; Razzaghi-Asl et al. 2017). Our results on isolated mitochondria obtained from human monocytes showed significant mitochondrial toxic changes such as mitochondrial swelling, inhibition of SDH, and cytochrome C release (Fig. 5a–c). Mitochondrial alterations have been associated with some forms of disorders

(Zapico and Ubelaker 2014). Additionally, our results suggest that the gradual and progressive occurrence of these alterations in exposed oncology drugs may play a role in progression of mentioned diseases.

Monocytes are central to the pathophysiology of inflammation. They have been found to be activated in rheumatoid arthritis (RA) (Davignon et al. 2012), and aberrations of monocyte phenotype and function are increasingly recognized in systemic lupus erythematosus (SLE) and animal models of the disease (Li et al. 2010). Therefore, presumably toxic compound such as TiO<sub>2</sub>-NPs could be effective in triggering of inflammatory conditions.

**Compliance with ethical standards** This study was approved by the Shahid Beheshti University of Medical Sciences research ethics committee, and all healthy individuals signed an informed consent form.

**Conflict of interest** The authors declare that there is no conflict of interest.

## References

- Böhme S, Stärk H-J, Meißner T, Springer A, Reemtsma T, Kühnel D, Busch W (2014) Quantification of Al<sub>2</sub>O<sub>3</sub> nanoparticles in human cell lines applying inductively coupled plasma mass spectrometry (neb-ICP-MS, LA-ICP-MS) and flow cytometry-based methods. *J Nanopart Res* 16(9):2592. <https://doi.org/10.1007/s11051-014-2592-y>
- Bradford MM (1976) A rapid and sensitive method for the quantitation of microgram quantities of protein utilizing the principle of protein-dye binding. *Anal Biochem* 72(1-2):248–254. [https://doi.org/10.1016/0003-2697\(76\)90527-3](https://doi.org/10.1016/0003-2697(76)90527-3)
- Cui Y, Gong X, Duan Y, Li N, Hu R, Liu H, Hong M, Zhou M, Wang L, Wang H (2010) Hepatocyte apoptosis and its molecular mechanisms in mice caused by titanium dioxide nanoparticles. *J Hazard Mater* 183(1-3):874–880. <https://doi.org/10.1016/j.jhazmat.2010.07.109>
- Davignon J-L, Hayder M, Baron M, Boyer J-F, Constantin A, Apparailly F, Poupot R, Cantagrel A (2012) Targeting monocytes/macrophages in the treatment of rheumatoid arthritis. *Rheumatology* 52:590–598
- Gheshlaghi ZN, Riazi GH, Ahmadian S, Ghafari M, Mahinpour R (2008) Toxicity and interaction of titanium dioxide nanoparticles with microtubule protein. *Acta Biochim Biophys Sin* 40(9):777–782. <https://doi.org/10.1093/abbs/40.9.777>
- Ghosh M, Bandyopadhyay M, Mukherjee A (2010) Genotoxicity of titanium dioxide (TiO<sub>2</sub>) nanoparticles at two trophic levels: plant and human lymphocytes. *Chemosphere* 81(10):1253–1262. <https://doi.org/10.1016/j.chemosphere.2010.09.022>
- Ghosh M, Chakraborty A, Mukherjee A (2013) Cytotoxic, genotoxic and the hemolytic effect of titanium dioxide (TiO<sub>2</sub>) nanoparticles on human erythrocyte and lymphocyte cells in vitro. *J Appl Toxicol* 33(10):1097–1110. <https://doi.org/10.1002/jat.2863>
- Hanot-Roy M, Tubeuf E, Guilbert A, Bado-Nilles A, Vigneron P, Trouiller B, Braun A, Lacroix G (2016) Oxidative stress pathways involved in cytotoxicity and genotoxicity of titanium dioxide (TiO<sub>2</sub>) nanoparticles on cells constitutive of alveolo-capillary barrier in vitro. *Toxicol in Vitro* 33:125–135. <https://doi.org/10.1016/j.tiv.2016.01.013>
- He Y-Y, Huang J-L, Block ML, Hong J-S, Chignell CF (2005) Role of phagocyte oxidase in UVA-induced oxidative stress and apoptosis in keratinocytes. *J Invest Dermatol* 125(3):560–566. <https://doi.org/10.1111/j.0022-202X.2005.23851.x>
- Hissin PJ, Hilf R (1976) A fluorometric method for determination of oxidized and reduced glutathione in tissues. *Anal Biochem* 74(1):214–226. [https://doi.org/10.1016/0003-2697\(76\)90326-2](https://doi.org/10.1016/0003-2697(76)90326-2)
- Hong J, Zhang Y-Q (2016) Murine liver damage caused by exposure to nano-titanium dioxide. *Nanotechnology* 27(11):112001. <https://doi.org/10.1088/0957-4484/27/11/112001>
- Hosseini M-J, Shaki F, Ghazi-Khansari M, Pourahmad J (2013) Toxicity of vanadium on isolated rat liver mitochondria: a new mechanistic approach. *Metallomics* 5(2):152–166. <https://doi.org/10.1039/c2mt20198d>
- Hussain S, Thomassen LC, Ferencati I, Borot M-C, Andreau K, Martens JA, Fleury J, Baeza-Squiban A, Marano F, Boland S (2010) Carbon black and titanium dioxide nanoparticles elicit distinct apoptotic pathways in bronchial epithelial cells. *Part Fibre Toxicol* 7:1
- Jin C-Y, Zhu B-S, Wang X-F, Lu Q-H (2008) Cytotoxicity of titanium dioxide nanoparticles in mouse fibroblast cells. *Chem Res Toxicol* 21(9):1871–1877. <https://doi.org/10.1021/tx800179f>
- Lai JC, Lai MB, Jandhyam S, Dukhande VV, Bhushan A, Daniels CK, Leung SW (2008) Exposure to titanium dioxide and other metallic oxide nanoparticles induces cytotoxicity on human neural cells and fibroblasts. *Int J Nanomedicine* 2008:533
- Li Y, Lee PY, Reeves WH (2010) Monocyte and macrophage abnormalities in systemic lupus erythematosus. *Arch Immunol Ther Exp* 58(5):355–364. <https://doi.org/10.1007/s00005-010-0093-y>
- Liu H, Ma L, Liu J, Zhao J, Yan J, Hong F (2010) Toxicity of nano-anatase TiO<sub>2</sub> to mice: liver injury, oxidative stress. *Toxicol Environ Chem* 92(1):175–186. <https://doi.org/10.1080/02772240902732530>
- Long TC, Tajuba J, Sama P, Saleh N, Swartz C, Parker J, Hester S, Lowry GV, Veronesi B (2007) Nanosize titanium dioxide stimulates reactive oxygen species in brain microglia and damages neurons in vitro. *Environ Health Perspect* 115(11):1631–1637. <https://doi.org/10.1289/ehp.10216>
- Natarajan V, Wilson CL, Hayward SL, Kidambi S (2015) Titanium dioxide nanoparticles trigger loss of function and perturbation of mitochondrial dynamics in primary hepatocytes. *PLoS One* 10(8):e0134541. <https://doi.org/10.1371/journal.pone.0134541>
- Razzaghi-Asl N, Seydi E, Alikhani R, Rezvani S, Miri R, Salimi A (2017) Synthesis and toxicity assessment of 3-oxobutanamides against human lymphocytes and isolated mitochondria. *Environ Toxicol Pharmacol* 51:71–84. <https://doi.org/10.1016/j.etap.2017.03.006>
- Rotem R, Heyfets A, Fingrut O, Blickstein D, Shaklai M, Flescher E (2005) Jasmonates: novel anticancer agents acting directly and selectively on human cancer cell mitochondria. *Cancer Res* 65(5):1984–1993. <https://doi.org/10.1158/0008-5472.CAN-04-3091>
- Salimi A, Ayatollahi A, Seydi E, Khomeisi N, Pourahmad J (2015a) Direct toxicity of amyloid beta peptide on rat brain mitochondria: preventive role of *Mangifera indica* and *Juglans regia*. *Toxicol Environ Chem* 97:1057–1070
- Salimi A, Roudkenar MH, Sadeghi L, Mohseni A, Seydi E, Pirahmadi N, Pourahmad J (2015b) Ellagic acid, a polyphenolic compound, selectively induces ROS-mediated apoptosis in cancerous B-lymphocytes of CLL patients by directly targeting mitochondria. *Redox Biol* 6:461–471. <https://doi.org/10.1016/j.redox.2015.08.021>
- Salimi A, Saharkhiz MP, Motallebi A, Seydi E, Mohseni AR, Nazemi M, Pourahmad J (2015c) Standardized extract of the Persian Gulf sponge, *Axinella sinoxea* selectively induces apoptosis through mitochondria in human chronic lymphocytic leukemia cells. *J Anal Oncol* 4:132–140
- Salimi A, Motallebi A, Ayatollahi M, Seydi E, Mohseni AR, Nazemi M, Pourahmad J (2016a) Selective toxicity of Persian gulf sea cucumber *holothuria parva* on human chronic lymphocytic leukemia b lymphocytes by direct mitochondrial targeting. *Environ Toxicol*
- Salimi A, Vaghar-Moussavi M, Seydi E, Pourahmad J (2016b) Toxicity of methyl tertiary-butyl ether on human blood lymphocytes. *Environ Sci Pollut Res* 23(9):8556–8564. <https://doi.org/10.1007/s11356-016-6090-x>
- Salimi A, Roudkenar MH, Seydi E, Sadeghi L, Mohseni A, Pirahmadi N, Pourahmad J (2017) Chrysin as an anti-cancer agent exerts selective toxicity by directly inhibiting mitochondrial complex II and V in CLL B-lymphocytes. *Cancer Investig* 35(3):174–186. <https://doi.org/10.1080/07357907.2016.1276187>
- Singh AK, Pandey P, Tewari M, Pandey HP, Shukla HS (2014) Human mitochondrial genome flaws and risk of cancer. *Mitochondrial DNA* 25(5):329–334. <https://doi.org/10.3109/19401736.2013.796520>
- Talari M, Seydi E, Salimi A, Mohsenifar Z, Kamalinejad M, Pourahmad J (2014) *Dracocephalum*: novel anticancer plant acting on liver cancer cell mitochondria. *Biomed Res Int* 2014:1–10. <https://doi.org/10.1155/2014/892170>

- Vahid A, Hadjati J, Kermanshah H, Ghabraei S (2004) Effects of cured dentin bonding materials on human monocyte viability. *Oral Surg, Oral Med Oral Pathol, Oral Radiol Endodontology* 98:619–621
- Vevers WF, Jha AN (2008) Genotoxic and cytotoxic potential of titanium dioxide (TiO<sub>2</sub>) nanoparticles on fish cells in vitro. *Ecotoxicology* 17(5):410–420. <https://doi.org/10.1007/s10646-008-0226-9>
- Wu P, Xie R, Imlay K, Shang JK (2010) Visible-light-induced bactericidal activity of titanium dioxide codoped with nitrogen and silver. *Environ Sci Tech* 44(18):6992–6997. <https://doi.org/10.1021/es101343c>
- Yu K-P, Huang Y-T, Yang S-C (2013) The antifungal efficacy of nano-metals supported TiO<sub>2</sub> and ozone on the resistant *Aspergillus niger* spore. *J Hazard Mater* 261:155–162
- Zapico SC, Ubelaker DH (2014) mtDNA mutations and their role in aging, diseases and forensic sciences. *Aging and Disease* 4:364–380
- Zhao J, Bowman L, Zhang X, Vallyathan V, Young S-H, Castranova V, Ding M (2009) Titanium dioxide (TiO<sub>2</sub>) nanoparticles induce JB6 cell apoptosis through activation of the caspase-8/Bid and mitochondrial pathways. *J Toxic Environ Health A* 72(19):1141–1149. <https://doi.org/10.1080/15287390903091764>